Journal of Alloys and Compounds 509 (2011) 7819–7825

Contents lists available at ScienceDirect

Journal of Alloys and Compounds

journal homepage: www.elsevier.com/locate/jallcom

Effects of synthesis, doping methods and metal content on thermoluminescence glow curves of lithium tetraborate

Mehmet Kayhan, Aysen Yilmaz*

Department of Chemistry, Middle East Technical University, Ankara 06531, Turkey

ARTICLE INFO

Article history:
Received 6 January 2011
Received in revised form 22 April 2011
Accepted 28 April 2011
Available online 7 May 2011

Keywords:
Lithium tetraborate
Synthesis
Doping
Characterization
Thermoluminescence

ABSTRACT

Lithium tetraborate: $Li_2B_4O_7$, (LTB) has been synthesized and doped with various Mn content by different methods, such as, high temperature solid state synthesis and solution assisted synthesis methods. Powder XRD results proved the formation of solid-solution by replacing Mn with Li ions in LTB lattice at lower amount of Mn doping, for example 0.1–3.0% Mn doping. In this research TL glow curves of Mn doped lithium tetraborate (LTB:Mn) produced by using different synthesis and doping methods and the effects of Ag, P and Mg as co-dopant were investigated. Structural and morphological analyses of products were done by using Fourier Transform Infrared spectroscopy (FTIR), Powder X-Ray Diffraction (XRD), Scanning Electron Microscopy (SEM), Transmission Electron Microscopy (TEM) and Raman Spectroscopy.

1. Introduction

Thermoluminescence dosimetry is an interesting research area for over the few past decades, especially in the fields of environmental, personal, and clinical radiation applications. Even though, for a long time many thermoluminescent (TL) materials are being used in radiation dosimetry, the topic is open for extensive research to get new TL materials having lower cost or better performance. Thermoluminescent dosimeter (TLD) needs to have some features such as; a simple glow curve structure, a high gamma ray sensitivity, low fading of TL signal, linear dose-response relationship, simple annealing procedure for reuse, chemical stability and inertness to extreme climatic variations, insensitive to daylight, suitable effective atomic number (Z_{eff}), close to that of soft tissue which is 7.42 [1]. None of the commercial dosimeters except for the one containing lithium tetraborate, $Li_2B_4O_7$, (LTB) are tissue equivalent. However, it is important that the dosimeter used to measure human exposure to radiation show similar atomic properties with human tissue. The effective atomic number of lithium tetraborate is (7.42), which is almost the same as that of the biological tissue [2].

Many researchers investigated the TL properties of LTB doped materials with different activators such as: Mn, Cu, Ag, and Mg [3–9]. The first thermoluminescent material based on LTB activated by Mn is commercialized by Harshaw under the name TLD-800. Kelemen et al. [2] reported the radioluminescence and thermoluminescence data for Mn doped single crystal and glassy samples of LTB, and single crystal form of the LTB:Mn was reported with a glow curve containing one peak at about 80 °C, and another peak at about 220 °C although glassy form had a very broad peak at about 150 °C. Wall et al. [10] investigated the suitability of three different thermoluminescent lithium borates; LTB:Mn, LTB:Cu and LTB:Cu,Ag. The properties of copper doped LTB powder make it more attractive for low dose measurements than manganese doped. However, the energy response of the copper doped material was not quite as suitable as that of the manganese doped material for measuring doses to tissue at photon energies lower than 100 keV. Driscoll et al. [11] compared the thermoluminescence properties of Mn doped LTB powder with Cu doped LTB and Cu and Ag doped LTB on their dose-response behaviors and degrees of fading and the results of this study fitted suitable well with the results of Wall. Lorrain et al. [12] doped transition elements including Mn and rare earths into LTB and compared the thermoluminescence results of doped LTB. Lorrain reported a LTB:Mn glow curve with one peak at about 100 °C and another peak at 235 °C which is produced by using a completely new doping method which is called Lorrain doping. Kitis et al. [9] reported a study on the kinetic parameters of LTB:Mn,Si, LTB:Cu, LTB:Cu,In and MgB_4O_7:Dy,Na [6]. Park et al. [13] compared the thermoluminescence and photoluminescence results of Cu, Mn and Mg doped LTB single crystals. LTB:Cu had a glow curve consisting of three peaks, one is at 125 °C, one is at 210 °C, and the other one is at about 260 °C. LTB:Mg gave a glow curve with only one peak at about 200 °C, although LTB:Mn gave a peak at about 250 °C. Holovey et al. [14] focused on the thermoluminescent behaviors with different

* Corresponding author. Tel.: +903 12210 5150; fax: +903 122103 200.
E-mail address: ayseny@metu.edu.tr (A. Yilmaz).

0925-8388/$ – see front matter © 2011 Elsevier B.V. All rights reserved.
doi:10.1016/j.jallcom.2011.04.137

annealing conditions of LTB:Mn single crystals. Tiwari et al. [15] studied the photoluminescence and thermoluminescence properties of single crystals of lithium tetraborate doped with Cu (0.5 wt%). Its TL sensitivity was found to be 3.3 and 0.06 times that of TLD-100 and TLD-500 respectively and a UV–vis transmission spectrum confirms the doping of Cu^+ ions in the crystal. Intense emission at 360 nm and single exponential decay (24.18 μs) strongly point to one type of Cu^+ ions as the emitting species.

In this research, it is aimed to see if there is any effect of synthesis and doping methods on TL glow curves of LTB:Mn products with different Mn contents in LTB. All four types of products, which are obtained by high temperature solid state synthesis and solution assisted synthesis method of lithium tetraborate and doped by the high temperature solid state doping method, and solution assisted doping method, showed different TL glow curves. High temperature solid-state synthesis and doping with powder forms of reactants had the most promising results in thermoluminescence measurements.

2. Experimental

Synthesis of LTB was done in two different ways; solution assisted (process-1) and high temperature solid-state reactions (process-2). In process-1, Li_2CO_3 and H_3BO_3 with a molar ratio of 1:4, dissolved in 15 ml distilled water by heating gently. After evaporating of extra water by heating without boiling, viscous transparent mixture was taken into crucibles and put into a furnace to heat up to 750 °C for 1 h. In process-2, Li_2CO_3 and H_3BO_3 with a molar ratio of 1:4 were mixed and grinded in an agate mortar. The mixture was put into a furnace to heat up to 400 °C for 3 h. The intermediate phase was grinded in an agate mortar and put into the furnace to heat up to 750 °C for 2 h.

Doping procedure was done in two different ways; solution assisted (process-1) and high temperature solid-state (process-2) doping. In process-1, the dopant chemicals were dissolved in distilled water and mixed with LTB. The suspension was put into a furnace in a crucible to heat up to 750 °C for 6 h. The product was then grinded finally. In process-2, LTB and the dopant chemical was mixed in an agate mortar and heated up to 750 °C for 6 h.

In the investigation of effects of synthesis and doping methods, a matrix of four combinations were applied: Solution assisted synthesis – solution assisted doping (process-1,1), solution assisted synthesis – high temperature solid state doping (process-1,2), high temperature solid state synthesis – solution assisted doping (process-2,1), high temperature solid state synthesis – high temperature solid state doping (process-2,2). Mn was chosen as the main dopant and $MnCl_2{\cdot}4H_2O$ was used as the Mn source. $AgNO_3$, $(NH_4)_2HPO_4$ and $MgCl_2{\cdot}4H_2O$ were used as co-dopant sources with varying dopant concentrations in the range of 0.1–10%.

The materials produced were characterized by XRD, FTIR and SEM methods. The characterization studies aimed at detection of any structural difference caused by doping operation besides confirmation of lithium borate in the correct form namely lithium tetraborate ($Li_2B_4O_7$), LTB.

The X-ray Diffractometer employed for the crystal structure investigations was a Rigaku MiniFlex X-ray Diffractometer with a radiation source of CuKα. The crystal structures of the lithium tetraborate were recorded within a 2θ range of 5–80°. The vibrational modes of the materials produced were studied by VARIAN 1000 FTIR spectrometer between wave numbers 400 and 4000 cm^{-1}. The morphological differences were determined by using QUANTA 400F Field Emission SEM with magnification between 12 and 900,000, variable pressure between 2 and 133 Pa, acceleration voltage of 0.1–30 kV. Microstructures of products were investigated by using transmission electron microscope (TEM). The samples for TEM observations were prepared by suspending the particles in ethanol by ultrasonification and drying a drop of the suspension on a carbon-coated copper grid. TEM was carried out employing JEOL 2100F electron microscope at 200 kV and pictures were taken by GATAN Orios 2 camera. Raman measurements were conducted by FT-RAMAN (FRA 106, YAG Laser) at 1064 nm wavelength. The actual amount of dopants in LTB was determined by using Perkin Elmer Optima 4300DV Inductively Coupled Plasma Optical Emission Spectrometer. Sample solution was prepared by using microwave oven.

The dosimetric properties of the samples were determined by using Harshaw TLD Reader Model 3500. The heating rate was chosen as the lowest possible for the measurements to be most reliable. As a result, the heating rate of 1 °C/s was used from 50 °C to 400 °C. The examined dosimeters were exposed to Beta, 90Sr–90Y radiations at room temperature for 5 min while the radiation given was 0.5 Gy/min. The sample amount was 10 mg which is within the reliable range determined. A standard clean glass filter was always installed in the reader between sample and photomultiplier tube. This filter allows the light whose wavelength is between ≈250 and ≈1000 nm to pass through it and thereupon eliminates unwanted infrared lights that are emitted from the heater.

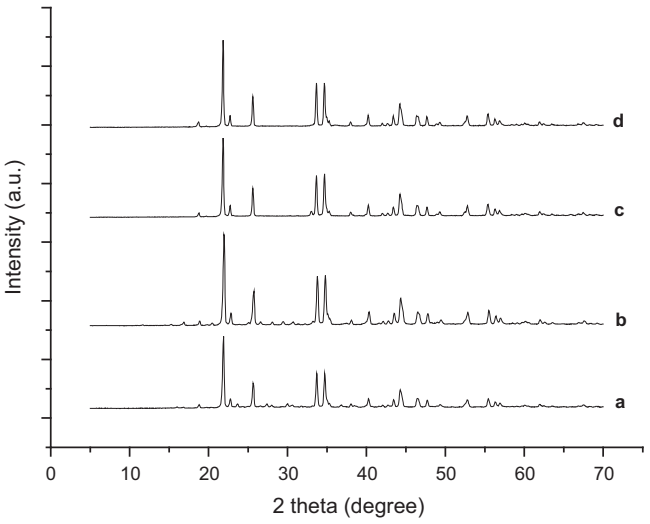

Fig. 1. XRD patterns of solution assisted synthesized undoped LTB (a), high temperature solid synthesized undoped LTB (b), solution assisted synthesized 1 wt% Mn doped LTB (c), and high temperature solid synthesized 1 wt% Mn doped LTB (d).

2.1. Results and discussions

XRD results (Fig. 1) revealed that LTB was successfully synthesized by both of the processes. Most intense peaks of the XRD pattern of LTB sample were assigned by the help of corresponding reference data [16]. LTB in tetragonal crystal structure with $I4_1cd$ space group and unit cell parameters are $a = 9.477$, $b = 9.477$, and $c = 10.286$ Å. In comparison of the synthesis methods, peak intensities and FWHM values of peaks and peak positions mainly were similar with each other. Also there was no other structural evidence belonging to impurities in XRD patterns up to 4.0% Mn doping. Effect of doping concentration on the lattice parameters have been observed as shift on the peak positions of different c parameters of Miller indices to higher 2θ values up to 4.0% Mn doping by weight. Above 4% Mn doped samples the peaks of Mn_2O_3 impurities were detected. In the lower concentrations of manganese doping, the only c parameters of unit cell were decreased: For 0.1 and 0.5% Mn the c parameter of unit cell were calculated as 10.252 Å, for 1.0, 2.0 and 3.0% Mn doped samples have larger unit cell dimension in c which were 10.269 Å. 4.0% Mn and higher weight of Mn doped samples have separation of phases and cell parameter of c dimension turned to pure LTB value which is 10.286 Å. These findings are reasonable; there are radii differences in between Li and Mn ions in four and six coordination: According to Shannon [17] Li^+ ion have 59 and 76 pm radii in four and six coordination, respectively. Mn^{2+} has 67 pm radii in six coordination and Mn^{4+} ion has 37 and 53 pm radii

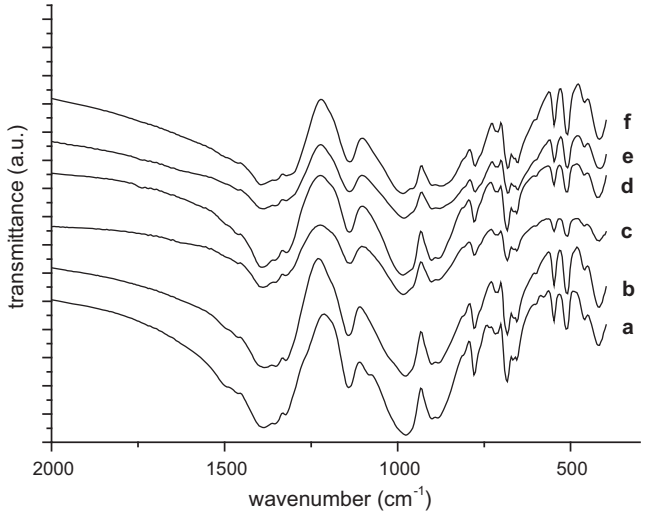

Fig. 2. FTIR spectra of solution assisted synthesized undoped LTB (a), high temperature solid synthesized undoped LTB (b), solution assisted synthesized and 1 wt% Mn solution assisted doped LTB (c), solution assisted synthesized and 1 wt% Mn high temperature solid doped LTB (d), high temperature solid synthesized and 1 wt% Mn solution assisted doped LTB (e), and high temperature solid synthesized and 1 wt% Mn high temperature solid doped LTB (f).

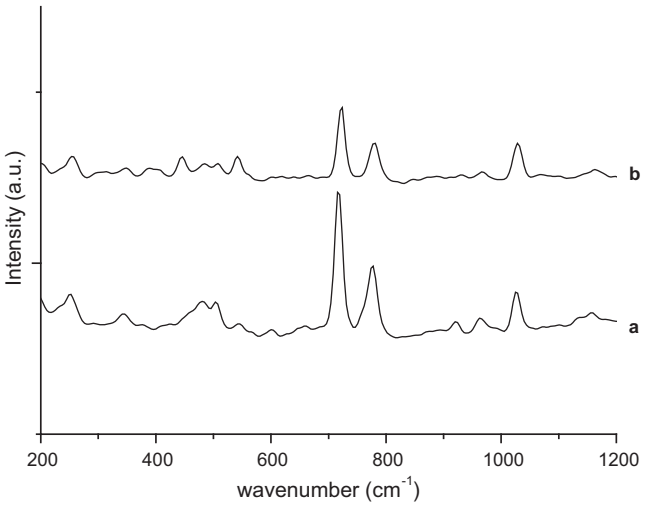

Fig. 3. Raman Spectra of LTB synthesized by solution assisted method (a) and high temperature solid-state method (b).

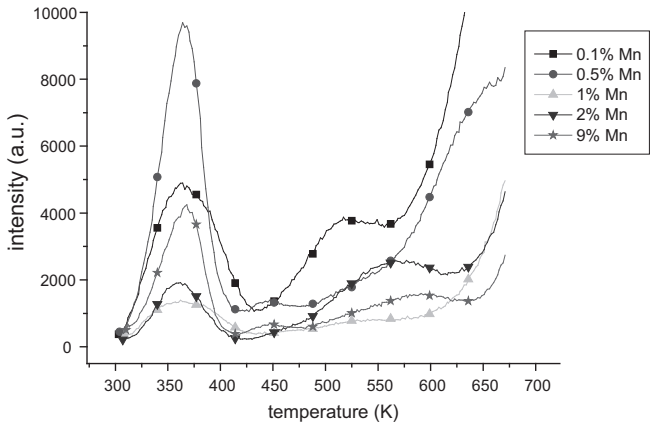

Fig. 5. Thermoluminescence measurements of LTB synthesized with solution assisted method and solution assisted doped with varying Mn content in the range of 0.1–10 wt%.

in four and six coordination, respectively, which are all smaller than Li^+ ion causes decrease in the *c* cell parameter when Li^+ ion replaced by Mn ions. In the variation of manganese content doped into lithium tetraborate, an increase is observed in the background with the increasing manganese percentage in LTB. The reason behind this is the fluorescence of Mn under Cu radiation since Cu source was used in XRD measurements. In order to prove the manganese content of samples which were prepared by different methods, ICP-OES elemental analysis was performed to only 1.0% Mn doped samples and the results proved the reliability of methods of doping: 1.0% Mn doped sample prepared by process-1,2 has 0.975 ± 0.003% Mn and process-2,2 sample 0.987 ± 0.005% Mn.

Also FTIR spectra of all doped and undoped samples well agreed with the XRD results about the Mn content (Fig. 2). All of the other bands were well fitted with the literature values for BO_3 and BO_4 ring structure vibrations. Asymmetric B–O stretching modes of planar BO_3^{3-} groups show bands in 1500–1200 cm^{-1} region. Bands in the 1100–940 cm^{-1} region are due to asymmetric and symmetric BO_4 stretching vibrations. There was a very weak band at 1080 cm^{-1} in Fig. 2(a) which was not observed in high temperature solid synthesized undoped or solution assisted and high temperature solid synthesized and doped products. This band was resulted from uncoordinated CO_3^{2-} vibrations [18].

Fig. 3 shows the Raman spectra of the solution assisted and high temperature solid synthesized LTB reveal that bands between 200 and 1200 cm^{-1} can be attributed to stretching for BO_4 tetrahedron and BO_3 planar triangle structures. Peak

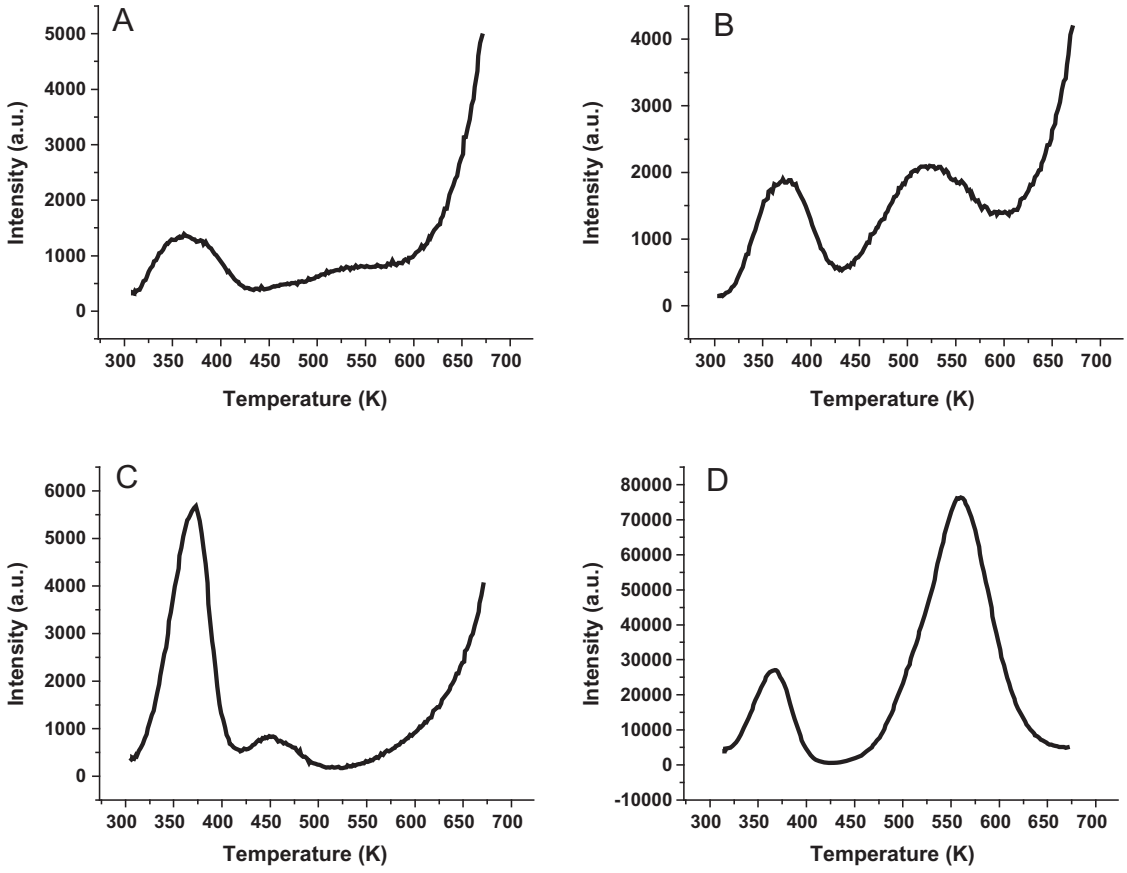

Fig. 4. Thermoluminescence measurements of solution assisted synthesized 1 wt% Mn solution assisted doped LTB (A), solution assisted synthesized 1 wt% Mn high temperature solid doped LTB (B), high temperature solid synthesized 1 wt% Mn solution assisted doped LTB (C), and high temperature solid synthesized 1 wt% Mn high temperature solid doped LTB (D).

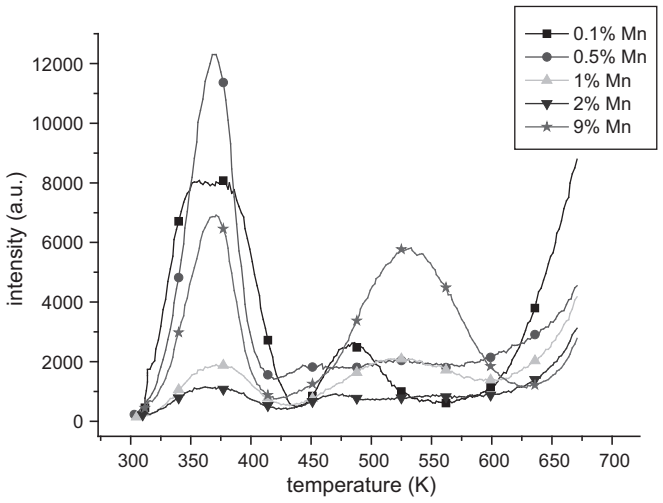

Fig. 6. Thermoluminescence measurements of LTB synthesized with solution assisted method and high temperature solid state doped with varying Mn content in the range of 0.1–10 wt%.

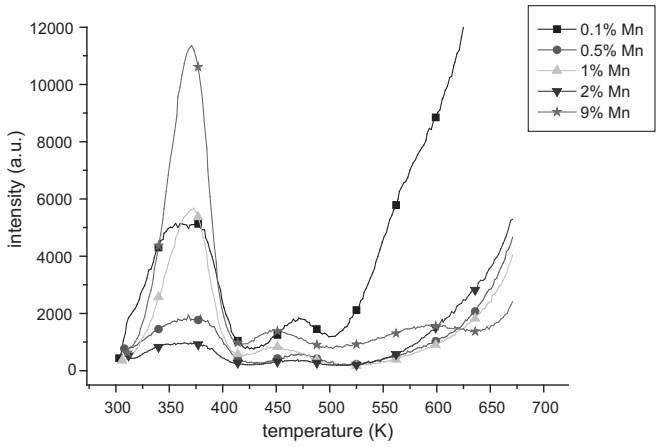

Fig. 7. Thermoluminescence measurements of LTB synthesized with high temperature solid state synthesis method and solution assisted doped with varying Mn content in the range of 0.1–10 wt%.

located around 256 cm^{-1} is attributed to ν_4 asymmetric stretching of BO_4. The bands between 344 and 504 cm^{-1} and bands between 1024 and 1156 cm^{-1} are assigned as ν_4 asymmetric stretching and ν_3 tetrahedral distortion of BO_4, respectively. The features seen around 921 and 966 cm^{-1} and between 658 and 777 cm^{-1} correspond to ν_1 triangular symmetric stretching and ν_4 triangular asymmetric deformation of BO_3 structure, respectively [6–9].

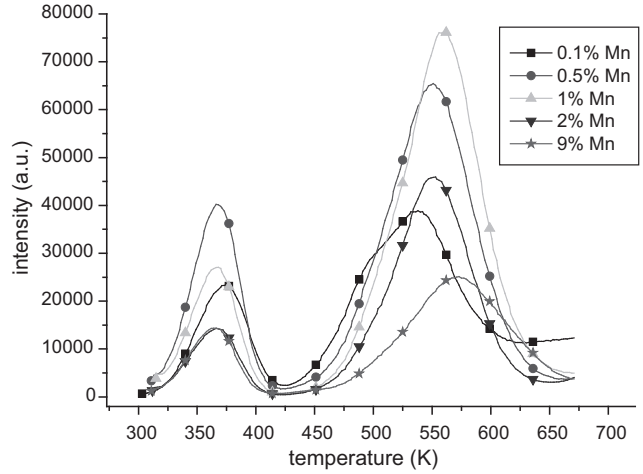

Fig. 8. Thermoluminescence measurements of LTB synthesized with high temperature solid state synthesis method and high temperature solid state doped with varying Mn content in the range of 0.1–10 wt%.

Thermoluminescence measurements of samples produced by different methods were performed and their glow curves are available in Fig. 4: The intensities of high temperature glow peak about 473–523 K are different between different synthesis and doping methods. In the literature there are reports on thermoluminescent performances of Cu, Ag, Mn and Cu with In (as co-dopant) doped LTB [19–25]. All of these materials gave a glow curve consisting of two glow peaks; the first one is at 383–393 K, and the second one in the range between 458 and 503 K, depending on the activator. Different shapes of glow curves for different synthesis and doping methods of LTB is in agreement with the data for Cu doped LTB, reported by Pekpak et al. Cu, Ag and Cu with In and Ag (as co-dopant) doped LTB is reported with good TL performances [26].

TLD glow curve of LTB:Mn samples of process-1,1 with varying Mn content shown in Fig. 5 indicate that glow curve consisting of one peak at about 373 K and a shoulder like low intensity peak at about 523 K and a final increase in background up to 673 K and higher temperatures in thermoluminescence measurements. The shape of the glow curve did not change in any of the compositions in the range of 0.1 wt% and 10 wt% Mn content in LTB. TLD glow curve of samples LTB:Mn samples of process-1,2 are available in Fig. 6. They had a similar glow curve with samples of process-1,1 with a small increase in 523 K peak. Also in this set of varying manganese content, all of the compositions gave the same shape of glow curves. In Fig. 7 there are TLD glow curve of LTB:Mn samples of process-2,1. These curves had a peak at 373 K and a lower intensity peak at about 453 K. The intensity of 373 K peak is 4 times higher than process-1,1 sample, and also a similar background increase at very high temperatures was observed. LTB:Mn samples process-2,2 gave a glow curve consisting of one peak at about 373 K like the other 3 types of products. But this time there was a very high intense peak at about 553 K respectively (Fig. 8). Although the shape of the glow curve did not change in any of the compositions in the range of 0.1 wt% and 10 wt% Mn content in LTB, the intensity of the main glow peak at 553 K increased with the increasing Mn content from 0.1 wt% to 1 wt%. Above 1 wt% Mn in LTB, this intensity decreased with the increasing Mn content regularly. Glow peak temperature is important for dosimetric purposes and a good dosimetric material should give a glow curve consisting of a single sharp peak at the range of 453–523 K,

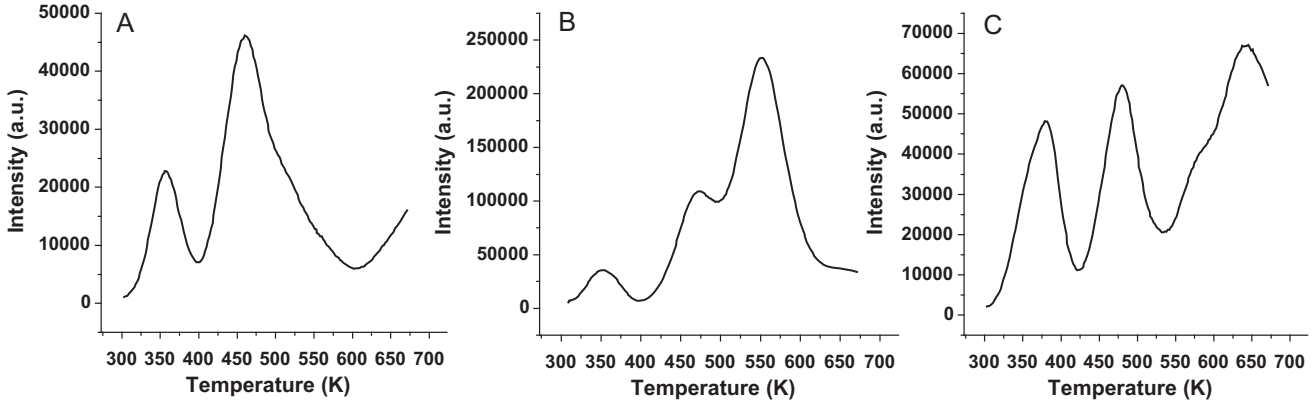

Fig. 9. Thermoluminescence measurements of LTB:Mn,Ag (A), LTB:Mn,P (B), and LTB:Mn,Mg (C).

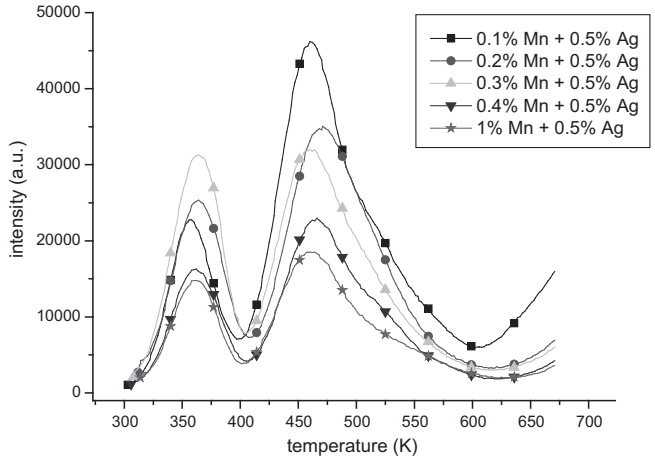

Fig. 10. Thermoluminescence measurements of LTB synthesized with high temperature solid state synthesis method and high temperature solid state doped with 0.5 wt% Ag and varying Mn content in the range of 0.1–1 wt%.

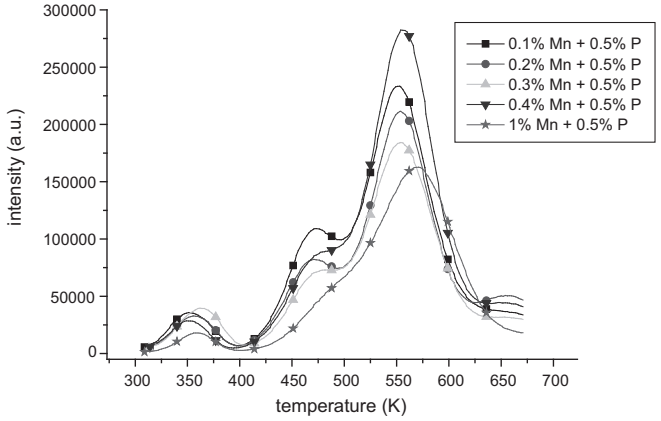

Fig. 11. Thermoluminescence measurements of LTB synthesized with high temperature solid-state synthesis method and high temperature solid-state doped with 0.5 wt% P and varying Mn content in the range of 0.1–1 wt%.

because peaks which are seen lower than 453 K fade and disappear quickly at about 1 day, and peaks at higher temperatures than 523 K the infrared emission from both TLD sample and the TLD holder may interfere [19]. The determination of trapping parameters such as order of kinetics, activation energy and frequency factor is also another important studies in the field of thermoluminescence properties of materials. For Mn doped lithium tetraborate samples, the trapping parameters of 583 K glow peak were studied by Manam and Sharma [28] by isothermal decay and Chen's method [29]. The results show that the frequency factor for this glow peak was found to be $3.7 \pm 0.77 \times 10^8\ s^{-1}$. The frequency factor represents the product of the number of times an electron hits the wall (in an attempt to escape from the potential well) and the wall reflection coefficient, treating the trap as a potential well (Fig. 9).

Since only process-2,2 samples gave a reasonably high intensity peak close to the usable temperature range, it is aimed to use these synthesis and doping methods to shift the peak at about 553 K to the usable range by adding co-dopants such as Ag, P and Mg. For all co-dopants, the amount used is 0.5 wt% of LTB and Mn content varied between 0.1 wt% and 1 wt%. Fig. 10 shows the TLD glow curve of co-activator containing lithium tetraborate samples such as Ag co-doped and Mn doped LTB gave a glow curve consisting of two peaks; one is at about 353 K and a higher intensity peak at 473 K. The best result with the highest intensity 473 K peak belongs to 0.1 wt% Mn and 0.5 wt% Ag content in LTB. Glow curve of P co-doped and Mn doped LTB (Fig. 11) has a peak at about 353 K, another peak at about 473 K and a higher intensity peak at 533 K. Although the high temperature peaks in these samples have higher intensities than LTB:Mn, Ag samples, these results are not better than LTB:Mn, Ag results since complexity in glow curves is not preferable in those materials. Also Mg co-doped and Mn doped LTB samples gave a complex glow curve (Fig. 12) consisting of four peaks; one is at about 373 K, one is at about 473 K, a shoulder at about 573 K and another peak at about 623 K. Recently, Xiong et al. [30] worked on to understand the role of Ag, indium and P dopant and co-dopants on LTB:Cu 0.02% phosphor to find concentration effect of co-dopants: According to their explanation, LTB consist of $[B_4O_9]^{6-}$ complex which has two trigonal planar BO_3 and two tetrahedral BO_4 units. The lithium ions are located at two different cites, oxygenic octahedrons and tetrahedrons. When metal ions doped into LTB, they enter into oxygenic octahedrons of tetrahedrons. The radii of Ag^+ is larger than Li^+ radius

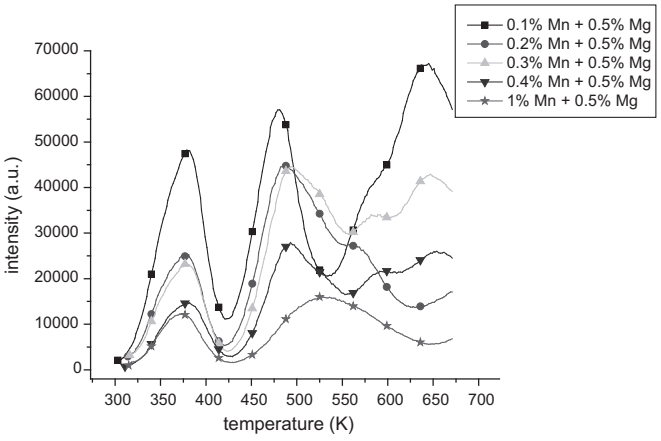

Fig. 12. Thermoluminescence measurements of LTB synthesized with high temperature solid state synthesis method and high temperature solid state doped with 0.5 wt% Mg and varying Mn content in the range of 0.1–1 wt%.

and LTB lattice will be destroyed, and therefore TL peaks are shifted. Phosphorus co-doping increased the peak intensities of glow curves because when P is doped into LTB, PO_4^{3-} can replace the BO_4 units, the radius of P is not too larger than boron atom, no destruction in LTB lattice would be expected. Electronegativity of P atom is higher than that of B atom, so impurity of P can produce electron traps in LTB crystals to enhance TL sensitivity. Mg^{2+} has approximately same ionic radii with Li^+ ions however, the high charge on Mg create great valance difference to destroy the LTB lattice.

Scanning electron microscopy (SEM) was done on the samples to monitor the surface morphology and the crystallite size of the samples. Fig. 13 shows the micrographs taken from undoped solution assisted synthesized and high temperature

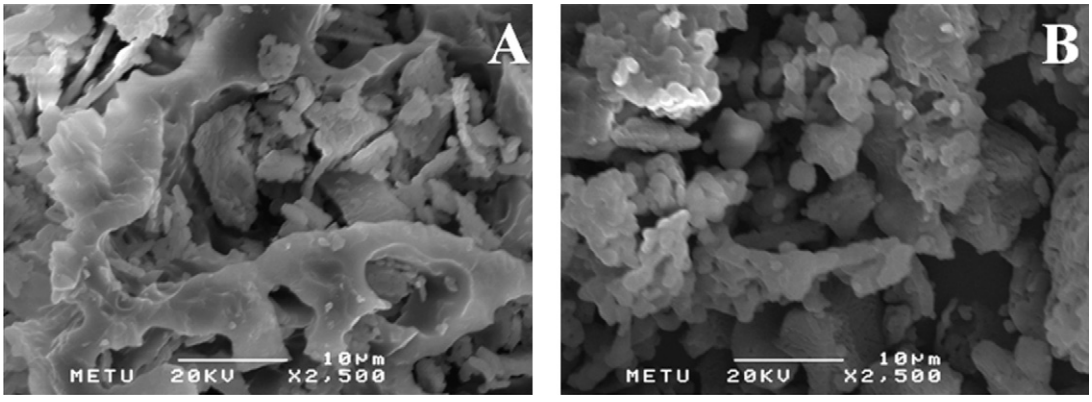

Fig. 13. SEM images of solution assisted synthesized undoped LTB (A) and high temperature solid synthesized undoped LTB (B).

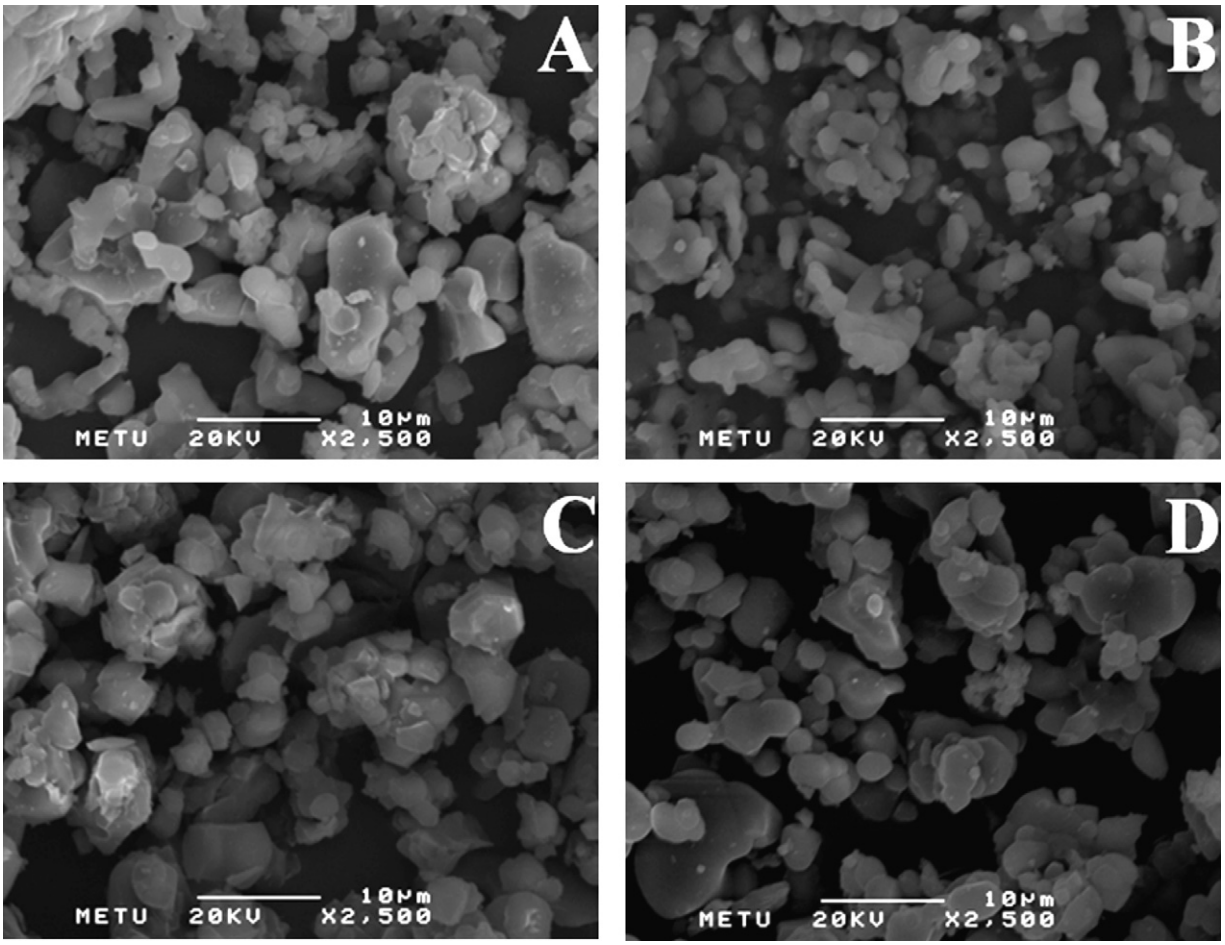

Fig. 14. SEM images of solution assisted synthesized 1 wt% Mn solution assisted doped LTB (A), solution assisted synthesized 1 wt% Mn high temperature solid doped LTB (B), high temperature solid synthesized 1 wt% Mn solution assisted doped LTB (C), and high temperature solid synthesized 1 wt% Mn high temperature solid doped LTB (D).

solid-state synthesized LTB samples. Solution assisted synthesized LTB has some melted or glassy structure without separate particle shapes, although high temperature solid state synthesized LTB has different sized crystalline particles. Particle size is not uniform according to SEM images of high temperature solid-state synthesized LTB samples. Although SEM images of solution assisted and high temperature solid-state synthesized undoped LTB samples seem different from each other, there are no significant morphological differences between four different types of products after doping. Agglomeration of particles and varying particle size can be seen in all four images (Fig. 14). In SEM images of Ag, P or Mg co-doped Mn doped LTB samples, still varying particle sizes and agglomeration of particles can be seen (Fig. 15).

Transmission electron microscopy (TEM) is a good tool to know local structure and microstructural morphology of the polycrystalline material [27]. TEM studies were conducted to compare the microstructure and crystalline size of the samples, which has different TLD glow curves. Fig. 16(a) and (b) shows the representative TEM bright field micrographs for samples both matrix synthesis and doping performed by high temperature solid-state method which has the best TLD glow curve and the sample prepared by solution assisted method and doped with Mn by high temperature solid state method, respectively. Both of the samples contain the same amount of activator (1% Mn). The micrograph shown in Fig. 16(a) is clearly indicating the presence of polycrystalline phase. Inset in Fig. 16(a) shows the corresponding selected area diffraction pattern (SAD). The irregularity of diffraction spots in SAD pattern indicates that the sample is not only one single crystal; it is formed by combination of more than one very well ordered crystallites. The particles are highly crystalline because the diffuse scatterings of spots are very bright. Fig. 16(b) is the

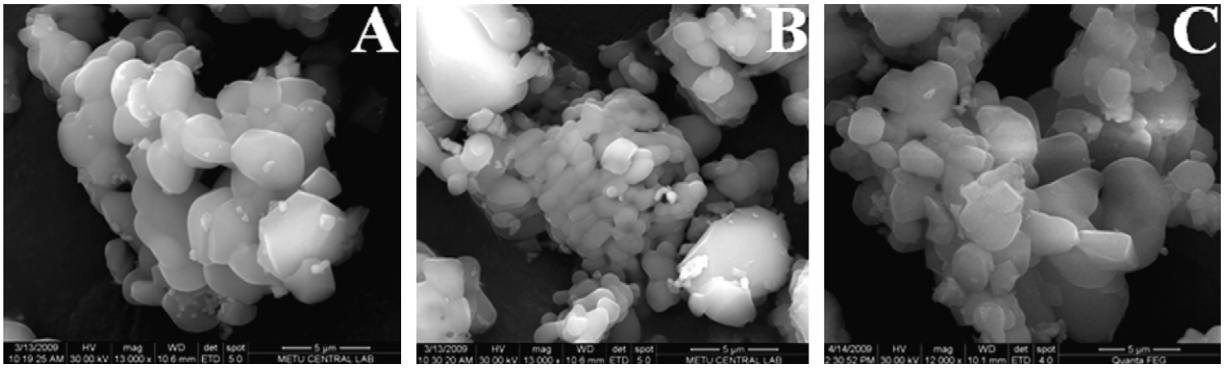

Fig. 15. SEM images of high temperature solid synthesized 1 wt% Mn 0.5 wt% Ag high temperature solid doped LTB (A), high temperature solid synthesized 1 wt% Mn 0.5 wt% P high temperature solid doped LTB (B), and high temperature solid synthesized 1 wt% Mn 0.5 wt% Mg high temperature solid doped LTB (C).

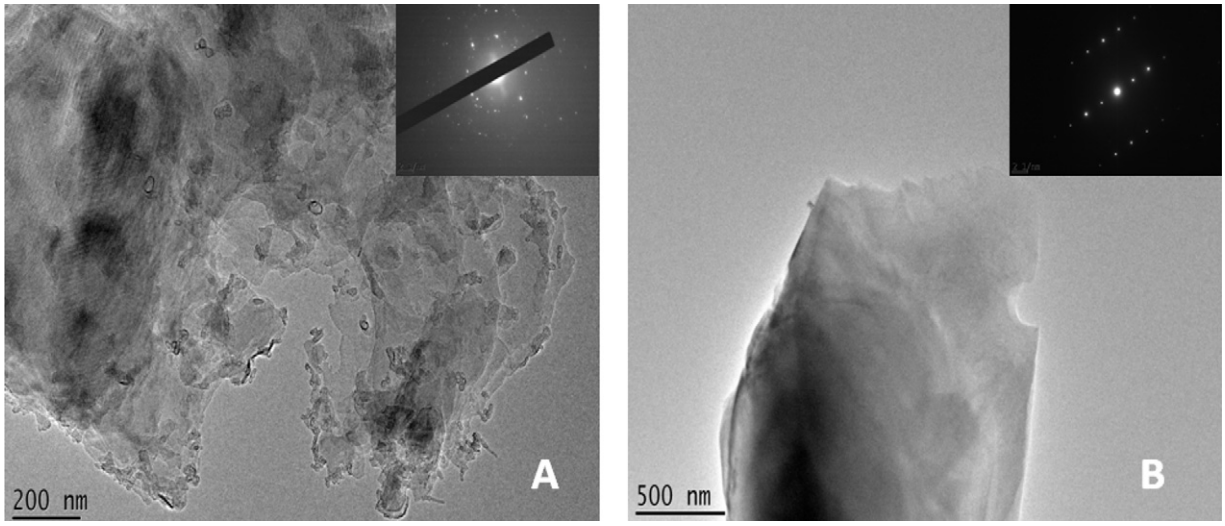

Fig. 16. TEM Micrograph taken from high temperature solid synthesized 1 wt% Mn high temperature solid doped LTB (A) and solution assisted synthesized 1 wt% Mn high temperature solid doped LTB (B).

micrograph of selected single crystal of sample, inset in Fig. 16(b) the corresponding SAD pattern: The clear spots in SAD pattern along with the diffuse rings are the indication of nanosize crystalline particles with single phase. Maybe these differences in microstructures of samples explain the differences in TLD glow curves: In order to obtain high intensity glow peak the sample need to be the combinations of nano sized crystallites. Having bigger single crystals reduces the glow peak intensity of sample. Preparing lithium tetraborate by solution assisted synthesis method helps the formation of bigger single crystals. High temperature solid-state synthesis method is the way to combine highly ordered crystalline nanoparticles of the same phase because this method has diffusion control step of reactants. This step increases the time duration during crystallization.

3. Conclusion

Thermoluminescence glow curves of Mn doped LTB produced by using different synthesis and doping methods were investigated. Solution assisted and high temperature solid-state synthesis methods with solution assisted and high temperature solid-state doping techniques were applied on LTB:Mn system. Powder XRD results proved the formation of solid-solution by replacing Mn with Li ions in LTB lattice at lower amount of Mn doping, for example 0.1–3.0% Mn doping. Although there was no change in the unit cell parameter of a dimension, there was decrease in the *c* unit cell dimension of host material due to the smaller ionic radii of Mn^{2+} than Li^{+} at four and six coordination number. Higher concentration of manganese in LTB caused the formation of impurity peaks of Mn_2O_3 in XRD pattern. High temperature solid-state synthesis of LTB and high temperature solid-state doping of Mn gave better glow curves with 1 wt% Mn content than other products with different synthesis and doping methods and than other percentages of Mn in LTB with two separable glow peak at 350 and 553 K with high intensity. The addition of Ag as co-dopant shifted the main glow peak to 473 K. P increased the intensity of glow peak at 553 K. Mg increased the glow curve complexity. In comparison of TEM micrographs of samples prepared by different methods, differences in their microstructures were observed: Solution assisted synthesis method produced bigger single crystals of lithium tetraborate containing manganese.

Acknowledgements

Authors want to acknowledge Prof. Dr. Necmeddin Yazici and Gaziantep University, and also BOREN for financial support for this study.

References

[1] A.S. Pradhan, Radiation Protection Dosimetry 1 (1981) 153–167.
[2] A. Kelemen, V. Holovey, M. Ignatovych, Radiation Measurements 43 (2008) 375–378.
[3] M. Ishii, Y. Kuwano, S. Asaba, T. Asai, M. Kawamura, N. Senguttuvan, T. Hayashi, M. Koboyashi, M. Nikl, S. Hosoya, K. Sakai, T. Adachi, T. Oku, H.M. Shimizu, Radiation Measurements 38 (2004) 571–574.
[4] J. Krogh-Moe, Acta Crystallographica 15 (1962) 190.
[5] G. Corradi, V. Nagirnyi, A. Kotlov, A. Watterich, M. Kirm, K. Polgár, A. Hofstaetter, M. Meyer, Journal of Physics: Condensed Matter 20 (2008) 025216 (9pp).
[6] G. Herzberg, Infrared and Raman Spectra of Polyatomic Molecules, van Nostrand, New York, 1945.
[7] A.F. Murray, D.J. Lockwood, Journal of Physics C: Solid State Physics 9 (1976) 3691–3700.
[8] G.L. Paul, W. Taylor, Journal of Physics C: Solid State Physics 15 (1982) 1753.
[9] G. Kitis, C. Furetta, M. Prokic, V. Prokic, Journal of Physics D: Applied Physics 33 (2000) 1252–1262.
[10] B.F. Wall, C.M.H. Driscoll, J.C. Strong, E.S. Fisher, Physics in Medicine and Biology 27 (1982) 1023–1034.
[11] C.M.H. Driscoll, E.S. Fisher, C. Furetta, R. Padovani, D.J. Richards, B.F. Wall, Radiation Protection Dosimetry 6 (1983) 305–308.
[12] S. Lorrain, J.P. David, R. Visocekas, G. Marinello, Radiation Protection Dosimetry 17 (1986) 385–392.
[13] K.-S. Park, J.K. Ahn, D.J Kim, H.K. Kim, Y.H. Hwang, D.S. Kim, M.H. Park, Y. Park, J.-J. Yoon, J.-Y. Leem, Journal of Crystal Growth 249 (2003) 483–486.
[14] V.M. Holovey, V.I. Sidey, V.I. Lyamayev, M.M. Birov, Journal of Physics and Chemistry of Solids 68 (2007) 1305–1310.
[15] B. Tiwari, N.S. Rawat, D.G. Desai, S.G. Singh, M. Tyagi, P. Ratna, S.C. Gadkari, M.S. Kulkarni, Journal of Luminescence 130 (2010) 2076–2083.
[16] International Centre for Diffraction Data (ICDD) card 18-0717.
[17] R. D. Shannon, Acta Crystallographica, A32, 751–767.
[18] A. Davydov, Molecular Spectroscopy of Oxide Catalyst Surfaces West Sussex, John Wiley & Sons Ltd., 2003, 135-292.
[19] C. Furetta, Handbook of Thermoluminescence, World Scientific Publishing, Singapore, 2003.
[20] J.H. Schulman, R.D. Kirk, E.J. West, Proc. 1st Int. Conf. Lumin. Dos., Stanford (USA), 1967.
[21] A. Moreno, C. Moreno, L. Archundia, Salsberg, Proc. 3rd Int. Conf. Lumin. Dos., Riso (Denmark), 1971.
[22] L. Botter-Jensen, P. Christensen, Acta Radiology (Suppl. 313) (1972) 247.
[23] M. Takenaga, O. Yamamoto, T. Yamashita, Proc. 5th Int. Conf. Lumin. Dos., San Paulo (Brazil), 1977.
[24] M. Takenaga, O. Yamamoto, T. Yamashita, Nuclear Instruments and Methods 175 (1980) 77.
[25] M. Takenaga, O. Yamamoto, T. Yamashita, Health Physics 44 (1983) 387.
[26] E. Pekpak, A. Yilmaz, G. Ozbayoglu, Journal of Alloys and Compounds, doi:10.1016/j.jallcom.2010.11.055.
[27] S. Kar, S. Verma, K.S. Bartwal, Journal of Alloys and Compounds 495 (2010) 288–291.
[28] J. Manam, S.K. Sharma, Radiation Effects and Defects in Solids 163 (2008) 813–819.
[29] R.S.W. Chen, S. McKeever, Theory of Thermoluminescence and Related Phenomena, World Scientific, Singapore, 1997.
[30] Z. Xiong, Q. Tang, X. Xiong, D. Luo, P. Ding, Radiation Measurements 46 (2011) 323–328.